



ELSEVIER

Contents lists available at SciVerse ScienceDirect

Talanta

journal homepage: [www.elsevier.com/locate/talanta](http://www.elsevier.com/locate/talanta)

Short communication

## Automated on-line preconcentration of trace aqueous mercury with gold trap focusing for cold vapor atomic absorption spectrometry

Mahitti Puanggam<sup>a</sup>, Purnendu K. Dasgupta<sup>b,\*</sup>, Fuangfa Unob<sup>a,\*</sup><sup>a</sup> Department of Chemistry, Faculty of Science, Chulalongkorn University, Payathai Road, Bangkok 10330, Thailand<sup>b</sup> Department of Chemistry and Biochemistry, The University of Texas at Arlington, Arlington 76019-0065, United States

## ARTICLE INFO

## Article history:

Received 1 March 2012

Received in revised form

24 May 2012

Accepted 24 May 2012

Available online 4 June 2012

## Keywords:

Mercury

Cold vapor atomic absorption spectrometry

Solid phase preconcentration

Gold trap

## ABSTRACT

A fully automated system for the determination of trace mercury in water by cold vapor atomic absorption spectrometry (CVAAS) is reported. The system uses preconcentration on a novel sorbent followed by liberation of the mercury and focusing by a gold trap. Mercury ions were extracted from water samples by passage through a solid phase sorbent column containing 2-(3-(2-aminoethylthio)propylthio)ethanamine modified silica gel. The captured mercury is released by thiourea and then elemental Hg is liberated by sodium borohydride. The vapor phase Hg is recaptured on a gold-plated tungsten filament. This is liberated as a sharp pulse (half-width < 2 s) by directly electrically heating the tungsten filament in a dry argon stream. The mercury is measured by CVAAS; no moisture removal is needed. The effects of chloride and selected interfering ions were studied. The sample loading flow rate and argon flow rates for solution purging and filament sweeping were optimized. An overall 50-fold improvement in the limit of detection was observed relative to direct measurement by CVAAS. With a relatively modest multi-user instrument we attained a limit of detection of 35 ng L<sup>-1</sup> with 12% RSD at 0.20 µg L<sup>-1</sup> Hg level. The method was successfully applied to accurately determine sub-µg L<sup>-1</sup> level Hg in standard reference water samples.

© 2012 Elsevier B.V. All rights reserved.

### 1. Introduction

Mercury is one of the most toxic elements but its unique attributes have made it difficult to find an alternative. The popularity of mercury-based energy efficient lamps and a variety of non-rechargeable batteries almost guarantee that even under the best of circumstances some of this mercury will find its way into the natural environment. There is also increasing use of coal as an energy source in a power-hungry planet, especially in developing countries. Widespread distribution and eventual deposition of mercury occurs via this route. There are many reviews on mercury in the environment and on the importance of its trace determination [1–5]. Lower and lower concentrations are necessary to be measured as our awareness of the omnipresence of the metal grows. Mercury is one of the only two metals that can be measured by atomic absorption spectrometry (AAS) or atomic fluorescence spectrometry [6] as the gaseous element at room temperature. This provides both matrix isolation and good sensitivity. The sensitivity is not enough, however, in AAS, the more affordable and the more widely used technique in the

developing world, to measure levels of mercury in most water samples of interest. Preconcentration has thus become the *sine qua non* for trace mercury determination. A comprehensive list of all papers that have reported on some form of mercury preconcentration is prohibitive: at the time of this writing, *Web of Science* returns 178 entries with *mercury* and *preconcentration* in the title and some > 1,300 entries with these in the “topic” coverage. Kerstin et al. [7] reviewed the preconcentration of mercury from natural waters in 2009. A non-exhaustive list of reported recent preconcentration media utilize itaconic acid [8], diphenylthiocarbazon [9], triisobutylphosphine sulfide [10], diphenylcarbazine [11] and gold [12] that are coated or bonded on various sorbents; just cation exchange resin can also be used [13]. Ionic liquids (IL's) increasingly find use for unrelated diverse problems; mercury preconcentration is no exception. IL's have been used for liquid–liquid extraction of mercury after forming a chelate [14] and in a more ingenious manner, as a single drop headspace microextractant [15]. There are several early reports of preconcentration by chelating mercury and preconcentrating the same on a standard hydrophobic sorbent, e.g., C-18 functionalized silica [16]; an attractive variant of this now simply uses a knotted PTFE coil, instead of a packed sorbent bed [17]. Functionalized nanosized sorbents [18,19] disperse in solution rapidly and provide for an interesting means of field preservation of samples without agitation; however, automated analysis of a large number

\* Corresponding authors.

E-mail addresses: Dasgupta@uta.edu (P.K. Dasgupta), Fuangfa.U@chula.ac.th (F. Unob).

of samples may not be facile. Considerable ingenuity has been shown to address the preconcentration problem: in one approach, the extractant is used at 50 °C, when it is a liquid. When the mixture is cooled, the extractant, containing the extracted Hg, floats up as a solid and can be picked up and transferred to an electrothermal analyzer [20]. The extraordinary affinity of gold for mercury has been known for a long time [21] and commercial thin gold film conductometric sensors for mercury [22,23] remain popular. More recently, sorption of mercury compounds in water on “active” gold surfaces have generated much interest, it has been shown that while Hg(0) is sorbed by a smooth gold surface, nanostructured gold surfaces capture both  $\text{Hg}^{2+}$  and  $\text{MeHg}^+$  [24,25].

For cold vapor atomic spectrometry of mercury, since the inception of the technique, it has been recognized that water vapor can limit the attainable limits of detection (LOD), especially if present in variable amounts [26,27]. While thermostating the measurement cell at an elevated temperature is the preferred solution for some manufacturers (see e.g., [www.mercury-instrumentsusa.com](http://www.mercury-instrumentsusa.com)) and alleviates the problem somewhat, the use of a dryer/drying tube is generally believed to provide superior results. However, this introduces potential questions of loss in the moisture removal device itself. When airborne mercury is preconcentrated on gold and later thermally desorbed [28], any variations in moisture content of the original sample becomes irrelevant, because matrix isolation has already been performed. Concentrating mercury and/or its compounds from aqueous samples directly on gold is possible as stated before but in this case one would need to rinse and dry the sorbent before thermal desorption is performed [24]. In addition, the thermal mass and configuration of a gold sorbent platform that can be deployed in the aqueous vs. gas phase are quite different; a much greater energy expenditure will likely be needed for thermal desorption of an aqueous phase solvent platform while a more rapid desorption should be possible for the former.

We propose that solution phase preconcentration on a sorbent, followed by liberation of Hg and refocusing by sorption and release from a low thermal mass gold platform provides the best of both worlds. The mercury sorbed by gold will be flashed off as a narrow pulse to determine the mercury with good sensitivity. Any type of liquid phase preconcentration should be applicable; we presently use 2-(3-(2-aminoethylthio)propylthio)ethanamine modified mesoporous silica. Some of the present authors previously reported this sorbent to have good selectivity and efficiency in capturing mercury over a wide range of pH (2–8) [29]. We do not, however, claim superiority over other sorbents that have been developed; no comparisons have been performed in this work. For the gold sorbent platform, we use a “coiled coil” tungsten filament (from a quartz-halogen lamp) electroplated with gold; such a device is very readily and inexpensively constructed. It is heated simply and rapidly with low power consumption and exhibits a very long life [28]. A fully automated system is presented.

## 2. Experimental

### 2.1. Instrumentation

An atomic absorption spectrometer (AAS, AAnalyst300, Perkin Elmer), flow injection system (FIAS-400) cold vapor mercury measurement system using a mercury hollow cathode lamp (N3050134) operated at 6 mA and a quartz absorption cell (B0507486, all from [www.perkinelmer.com](http://www.perkinelmer.com)) maintained at 200 °C, were used. Absorbance of mercury was measured at 253.7 nm with a 0.7 nm spectral band pass. High purity Argon

(99.999%) was used as the carrier gas for mercury vapor introduction to the cell.

### 2.2. Reagents and solutions

Standard metals solutions were prepared daily by appropriate dilution of stock metal solutions (Hg(II), Ag(I), Au(III) and Pb(II), 1000 mg L<sup>-1</sup>, BDH SpectroSol<sup>®</sup>) with 1% (w/v) H<sub>2</sub>SO<sub>4</sub> (Merck) in Milli-Q water. A solution of 1% (w/v) H<sub>2</sub>SO<sub>4</sub> in Milli-Q water was used as the carrier. Thiourea (BDH SpectroSol<sup>®</sup>) in 1% (w/v) H<sub>2</sub>SO<sub>4</sub> was used to elute retained mercury from the preconcentration column and prepared daily. This solution is referred to as the eluent. A NaBH<sub>4</sub> solution (5% w/v) stabilized with 0.2 M NaOH (both from Merck) was used to generate elemental mercury; this is referred to as the reductant. The accuracy of the method was validated with certified reference water samples (HG95-3, HG95-10, obtained from Environment Canada's National Water Research Institute, [www.ec.gc.ca](http://www.ec.gc.ca)).

### 2.3. Fabrication of the automated sample preconcentration and cold vapor introduction systems

Silica gel was modified with 2-(3-(2-aminoethylthio)propylthio)ethanamine as previously described [29] and used for solution phase preconcentration. The gold plated filament was prepared similar to that described in [28]. The filament was of the coiled coil type, 27 mm long, with a coil diameter of 2 mm and the diameter of the quartz envelope was 5.5 mm.

#### 2.3.1. Analysis system

The system is schematically shown in Fig. 1. The syringe pump (P/N 55022) equipped with an 8-port selector valve (P/N 17877) and a 10.0 mL syringe (P/N 19110, all from [www.kloehn.com](http://www.kloehn.com)) was used for solution delivery. The pump could store the entire operating program in its own memory and the cycle could be initiated by a TTL signal from the FIAS-400 via a software controlled relay. The pump also sent the TTL output signals in a programmed manner to a 8-bit PIC microcontroller (and associated circuits, 16F648A, Microchip, [www.es.co.th](http://www.es.co.th)) that controlled the solenoid valves (V1–V4) and powered the gold plated filament (GF) for thermal desorption at appropriate times. The microcontroller was programmed by MPLAB IDE software (V8.56, [www.microchip.com](http://www.microchip.com)). The elemental mercury generation and gas-liquid separation chamber was a custom made conical bottom glass tube G (1.5 cm i.d., 5.0 cm long), provided with an exit tube at the bottom and a neoprene stopper at the top. The preconcentration column (PCC) consisted of 30 mg of the functionalized sorbent packed in a 4.8 mm i. d. 25 mm long PTFE tube provided with custom-cut 20 μm PTFE frits (P/N 57185, [www.sial.com](http://www.sial.com)) and two PTFE adapters (B0196857, Perkin-Elmer). The solenoid valves (12VDC, 01540-11, [www.coleparmer.com](http://www.coleparmer.com) and 225T031, [www.nresearch.com](http://www.nresearch.com)) were 3-way valves with all PTFE contact parts with the exception of V1 (003-0636-900, [www.parker.com](http://www.parker.com)) which was a 3-way valve, operated in the 2-way mode. The system communication hierarchy is schematically shown in the supporting information (Fig. S1).

#### 2.3.2. Operation

Details are given in the supporting information, Table S1. PCC was first washed with Milli-Q water (MQW, 10 mL, syringe aspirate/dispense flow rates were 10 mL min<sup>-1</sup> except as stated). The syringe was washed with the sample and 10 mL sample was pumped through the PCC at different test flow rates (to test for capture efficiency). The syringe was then washed with 5 mL MQW and filled with 5 mL MQW. V1, normally open, was then turned

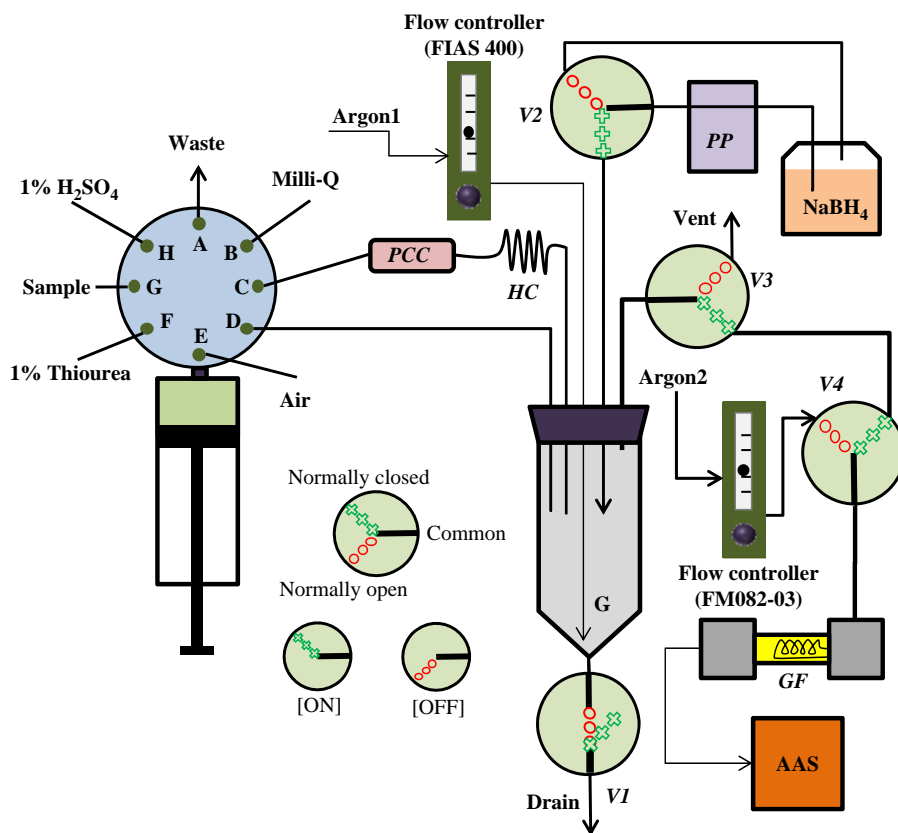


**Fig. 1.** Schematic diagram of system using liquid phase pre-concentration on solid sorbent and gold trap focusing. PCC: pre-concentration column, HC: holding coil (holds eluted Hg before delivering to reduction chamber G), PP: peristaltic pump, V1–V4: solenoid valves (inset shows ON/OFF port connections), G: reduction chamber-gas/liquid separator, GF: gold filament trap, AAS: Atomic Absorption Spectrometer.

on to seal off gas/liquid separator (G) bottom. The PTFE holding coil HC (25 cm, 3.2 mm o. d., 1.59 mm i. d.) was washed with 5 mL MQW into G. Air (2 mL) was aspirated into the syringe, V3 was off and vented, V1 was then turned off and the air dispensed into G to wash it out. The elution step began next. V1 was turned on to shut bottom of G. The syringe was washed with 0.5 mL eluent and then loaded with 0.5 mL eluent that was pumped through PCC into G at  $1 \text{ mL min}^{-1}$ . The syringe was filled next with 1.0 mL of the 1%  $\text{H}_2\text{SO}_4$  wash solution, which was also pumped through PCC into G. The reduction step began next. V3 and V4 were turned on so that any gaseous effluent from G proceeded through gold trap (GF). (Note that the lowest calibrated argon flow rate on the FIAS 400 is  $50 \text{ cm}^3 \text{ min}^{-1}$  and the FIAS-400 unfortunately has no capability of turning this flow on and off; hence it was always on.) The reductant was delivered through a separate peristaltic pump PP (part of the FIAS-400) that was turned on briefly before reductant delivery. It recirculated the reductant solution continuously through V2. When V2 was actuated ON, 0.50 mL of the reductant was delivered into G. The  $\text{Hg}^0$  generated initially was carried by the generated  $\text{H}_2$  and argon flow 1 to GF. GF chamber had dimensions of 0.5 cm i. d., 4.2 cm long. Once the reductant delivery was complete, V2 and PP were shut off, V3 was on for 70 s allowing the Hg-bearing purged gas to flow over GF. It has long been known that the presence of moisture does not affect the adsorption of Hg on gold [30], so no effort was made to remove the moisture. During this time the syringe was washed with the acid solution. V4 was now switched and argon flow 2, controlled by a flow controller (FM082-03, AALBORG instruments) at  $30 \text{ cm}^3 \text{ min}^{-1}$  flowed over GF. After 10 s to remove any residual moisture, the filament was powered (12 VDC) for 15 s and the released mercury signal was detected. During this time, G was

alternately washed with MQW and water to make it ready for the next sample.

All data collection and processing were done by Perkin Elmer software provided with the instrument. Some comparative experiments were conducted without the GF trap, with minor appropriate modifications to the system, directly introducing the liberated Hg to the AAS, via a soda-lime cartridge to remove the moisture; see Fig. S2 and Table S2.

#### 2.4. Method development, robustness and method validation

Certain parameters including the argon flow rate and the sample flow rate were investigated and optimized by analyzing standard mercury solutions ( $0.5$  and  $5.0 \mu\text{g L}^{-1}$ ). The robustness of the method was examined by monitoring the deviation of the calibration slope over 10 days ( $n=5$  each). Method validation was carried out by analyzing the certified reference water standards.

### 3. Results and discussion

#### 3.1. Choice of peak height vs. peak area for quantitation

Quantitation in AAS is typically done by peak area integration (especially in electrothermal atomization); however, in CVAAS measurement of Hg, peak height measurement is often used, whether without [16,31–37] or with [38–40] a gold trap. Kan et al. [41] examined CVAA for Hg both without and with a gold trap. Height measurement provided 3.3 and  $5 \times$  better LOD than area measurement for without and with a gold trap, respectively. Perkin-Elmer Corp. markets an Au–Pt “amalgam system” for the

preconcentration of Hg; they report only height-based quantitation for its use [42]. We therefore adopted height-based measurement in this work.

The limit of detection (LOD) was taken to be that signal which was three standard deviations of the baseline higher than the reagent blank signal itself; if baseline fluctuations follow a normal distribution, this would provide a 99% probability that at this level the signal is not due to baseline fluctuations; this largely follows the method detection limit calculations of the USEPA [43].

### 3.2. Initial work with first stage preconcentration only

Some of the initial experiments (effects of sample loading rate, chloride concentration, interference by selected metals) were conducted without the gold trap using the simplified arrangement shown in Fig. S2 in the supporting information. Our primary objective was to devise a protocol that will comfortably measure mercury levels of concern in tap water and drinking water in Thailand where the regulatory limit is set at  $1 \mu\text{g L}^{-1}$ . To quantitate reliably at this level, a fivefold lower LOD of at least  $0.2 \mu\text{g L}^{-1}$  was sought. The objective of our optimization efforts was thus to achieve an LOD of at least  $0.2 \mu\text{g L}^{-1}$  while achieving the maximum possible sample throughput rate. In preconcentration methods, aside from other parameters that affect the performance, the concentration LOD typically decreases in direct proportion to the volume of the sample preconcentrated; however, increasing the sample volume preconcentrated also requires more processing time. Based on initial experience with the total processing time, we arbitrarily set the sample volume to be 10.00 mL (this would lead eventually to a total analytical cycle time of 15 min, see Table S1).

The effect of the argon purge flow ( $50, 100, 150 \text{ cm}^3 \text{ min}^{-1}$ ) through the solution was studied in the system without the gold trap first. The net peak height obtained with standard mercury solutions ( $0.5$  and  $5.0 \mu\text{g L}^{-1}$ ) showed no significant dependence on this flow rate. The FIAS-400 did not allow for argon flow rates  $< 50 \text{ cm}^3 \text{ min}^{-1}$  where the flow rate will be known. An argon flow of  $50 \text{ cm}^3 \text{ min}^{-1}$  was henceforth used for purging the solution.

#### 3.2.1. Effect of sample loading rate

The sample loading flow rate must have an optimum as mercury capture efficiency may be incomplete at very high flow rates (pressure drops may also become prohibitive) while analysis time would increase with decreasing flow rates. Sample loading rates of  $3.0, 5.0$  and  $7.0 \text{ mL min}^{-1}$  were studied at two different mercury concentrations ( $0.5$  and  $5 \mu\text{g L}^{-1}$ ). The signal intensities were statistically indistinguishable (see Fig. S3) between loading rates of  $3.0$  and  $5.0 \text{ mL min}^{-1}$  while a discernible decrease occurred at a flow rate of  $7.0 \text{ mL min}^{-1}$ , with an attendant increase in standard deviation likely due to high back pressure. A loading rate of  $5.0 \text{ mL min}^{-1}$  was henceforth used.

#### 3.2.2. Effect of chloride concentrations

It is known that mercury(II) forms a stable chloro complex and chloride ion concentrations in natural waters can vary considerably. It was of interest to know if high levels of chloride would reduce the preconcentration efficiency and thus the signal. What we noted was unanticipated: compared to no chloride added, the calibration slope increased by 11.5% upon  $10 \text{ mg L}^{-1}$  chloride addition ( $0\text{--}5 \mu\text{g L}^{-1} \text{ Hg}^{2+}$  preconcentrated, see data in Fig. S4). We believe that this is caused by adsorptive loss of very low concentrations of Hg to glass containers used for making diluted standards (that is prevented by the presence of chloride and the formation of the chloro complex) rather than any systemic

behavior. This hypothesis is reinforced by the fact that even direct measurements (necessarily at a higher concentration range of  $0\text{--}100 \mu\text{g L}^{-1}$ ) showed a 3% increase in the calibration slope (see Fig. S5) upon  $10 \text{ mg L}^{-1}$  chloride addition (a lesser difference will indeed be expected, the loss is likely to be less than first order with concentration) and the fact that further increases in chloride concentration, all the way to  $1000 \text{ mg L}^{-1}$ , showed no further effect on the calibration slope. The presence of some amount of chloride in samples would thus seem to be beneficial. The majority of samples are likely to already have a chloride content greater than  $10 \text{ mg L}^{-1}$ . In the US, where extensive data are readily available, of 3425, 3938 and 2161 surface water samples analyzed in 2009, 2010 and 2011, 70, 70, and 72% of the samples respectively contained  $> 10 \text{ mg L}^{-1}$  chloride. Similarly, of 4147, 4817 and 3200 groundwater samples analyzed in the same years, 59, 63, and 66% of the samples contained  $> 10 \text{ mg L}^{-1}$  chloride [44]. In any case, small amounts of acid and/or bactericides like  $\text{CHCl}_3$  are typically added immediately to water samples after field collection and it would be a simple matter to add enough chloride to such preservatives that the overall chloride concentration will exceed  $10 \text{ mg L}^{-1}$ .

#### 3.2.3. Effect of interfering ions

Previous work [29] had shown that beyond Hg, the thiol-bearing sorbent used here has primary affinity for the soft acid metals, notably (Au, Ag, and Pb); the effect of these ions on mercury determination was investigated. Au (III), Ag (I) and Pb (II) ions were individually added into mercury (II) standards ( $1.00$  and  $4.00 \mu\text{g L}^{-1}$ ) at concentration of  $10, 25, 50$  or  $100 \mu\text{g L}^{-1}$ . The results are shown in Table 1 and indicate that at least up to  $50 \mu\text{g L}^{-1}$ , no significant interference is posed by Au or Pb while Ag interferes at all concentrations. The reason becomes apparent at higher concentrations of silver: Upon addition of the reductant, the solution visibly turns dark due to the formation of colloidal Ag, which doubtless binds the liberated Hg as the amalgam, inhibiting its release from solution. The fact that similar behavior is not observed with Au is likely because Au(III) is present as an anionic complex and is never captured in the first place (no color from a gold sol is seen). Silver in any meaningful concentrations are not likely to be present in any natural waters.

#### 3.2.4. Performance summary of single stage preconcentration

In this method, the analytical linear dynamic range was in the range of  $0.50\text{--}5.00 \mu\text{g L}^{-1}$ . The LOD, based on the standard deviation of the reagent blank was  $0.24 \mu\text{g L}^{-1}$  and did not meet

**Table 1**  
Effect of interfering ions on the recovery of mercury.

Metals ion	Concentration ( $\mu\text{g L}^{-1}$ )	$1.00 \mu\text{g L}^{-1}$ of Hg (II)		$4.00 \mu\text{g L}^{-1}$ of Hg (II)	
		(%) recovery	(%) RSD	(%) recovery	(%) RSD
Ag(I)	10	87	12	80	3.3
	25	54	20	58	4.5
	50	50	21	39	6.8
	100	40	27	37	7.2
Au(III) ( $\text{AuCl}_4^-$ )	10	99	11	101	2.7
	25	99	11	100	2.5
	50	86	12	100	2.5
	100	59	22	99	2.6
Pb(II)	10	99	13	102	2.8
	25	103	10	100	2.5
	50	94	10	100	2.5
	100	66	16	99	2.6

the initial goal of attaining an LOD of  $\leq 0.2 \mu\text{g L}^{-1}$ . Focusing on the gold trap was added to the system.

### 3.3. Solid phase preconcentration in combination with gold trap

#### 3.3.1. Effect of purge argon flow rate (argon flow 1)

The purge argon flow rate controls the rate at which liberated  $\text{Hg}^0$  flows over the gold filament and hence affects the ability of the latter to capture the  $\text{Hg}^0$ . Previous experiments with a gold filament platform [28] (but with a cell containing two filaments) indicated that a significant fraction was collected even at a flow rate of  $6000 \text{ cm}^3 \text{ min}^{-1}$ . In the present case, we assumed that at a flow rate of  $50 \text{ cm}^3 \text{ min}^{-1}$ , we would be collecting the liberated  $\text{Hg}^0$  nearly quantitatively. Since the limitations of the FIAS-400 did not allow us to test a flow rate any smaller than  $50 \text{ cm}^3 \text{ min}^{-1}$ , we deemed that ultimate performance rather than exact collection efficiency will be a better test. However, on the addition of  $\text{NaBH}_4$ , gaseous  $\text{H}_2$  is also evolved. From the amount of  $\text{NaBH}_4$  added, it can be computed that  $\sim 65 \text{ cm}^3$  of  $\text{H}_2$  is formed. Depending on how rapidly it is evolved, the passage of the main  $\text{Hg}^0$  bearing bolus over the gold filament can be faster than that estimated from a purge flow rate of  $50 \text{ cm}^3 \text{ min}^{-1}$  with an attendant decrease in collection efficiency. This aspect will benefit from further investigation in future studies of similar systems.

#### 3.3.2. Effect of argon flow rate during desorption

Once the filament is heated, as indicated in Fig. 1, argon flow 2 carries the evolved  $\text{Hg}$  to the detector; predictably, dilution decreases with a smaller flow rate and the signal height increases. Dilution is proportional to the flow rate; if this was the only factor that governed the signal height, it will decrease linearly with increasing flow rate (or increase linearly with reciprocal flow rate). However, the  $\text{Hg}$  is desorbed over a finite time period and gas phase diffusion is fast, the gain in peak height from reducing the flow rate is not linear because of diffusive broadening. The signal peak height exponentially reaches a plateau value as the reciprocal carrier flow rate (proportional to residence time) decreases. In fact, the peak full width half maxima (FWHM) do not markedly change with the carrier flow rate. Based on the data in Fig. 2, we chose an argon flow rate of  $30 \text{ cm}^3 \text{ min}^{-1}$ . Note that the carrier flow was begun and continued for 10 s to ensure that residual moisture in GF compartment was removed before heating the filament; this prolongs the lifetime of the filament. We observed no signal on a second firing of the filament, indicating quantitative desorption.

#### 3.3.3. Improvement of signal peak shape

Fig. 3 shows the system output with 1.0, 3.0 and  $5.0 \mu\text{g L}^{-1}$   $\text{Hg}$  with and without the gold trap. The use of the gold trap provides a much sharper, nearly Gaussian peak shape compared to that without it. Without the gold trap, the FWHM vary and increase with decreasing concentrations, but are between 3.5 to 4 times greater than those with the use of the gold trap. The latter system has an FWHM of  $< 1.9 \text{ s}$ , showing the rapidity of the desorption from the filament. The inset shows the trace for a  $150 \text{ ng L}^{-1}$  sample, processed with a 20 point moving average filter.

#### 3.3.4. Performance

The system with the gold trap exhibited a linear dynamic range of  $0.15$  to  $5.0 \mu\text{g L}^{-1}$  and an LOD of  $0.035 \mu\text{g L}^{-1}$ , meeting our original goal. Better LODs have been reported in the literature, especially for dedicated CVAA instruments. However, our instrument was a multipurpose multi-user instrument and far from the state-of-the-art. The lamp we used had a limited intensity and direct cold vapor determination provided an LOD of  $1.8 \mu\text{g L}^{-1}$ .

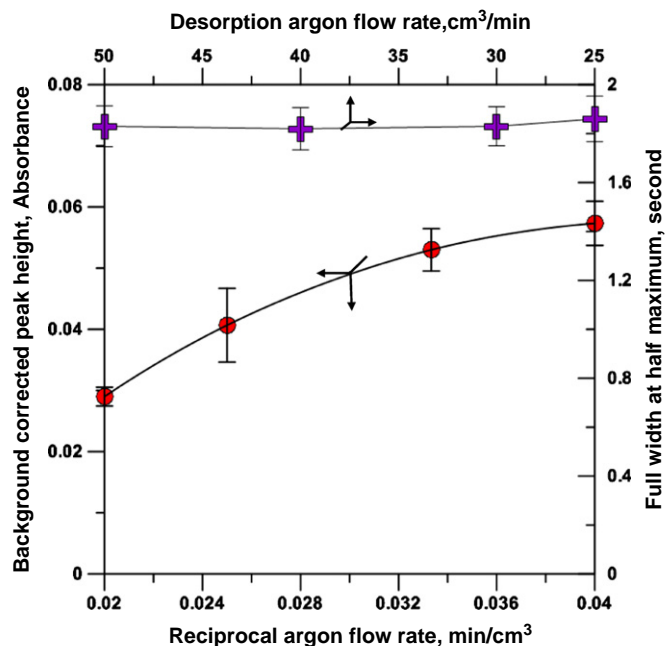


Fig. 2. Effect of argon carrier flow rate in the determination of mercury ( $0.50 \text{ mg L}^{-1}$ ) (Argon 2, Fig. 1) and relative constancy of peak width.

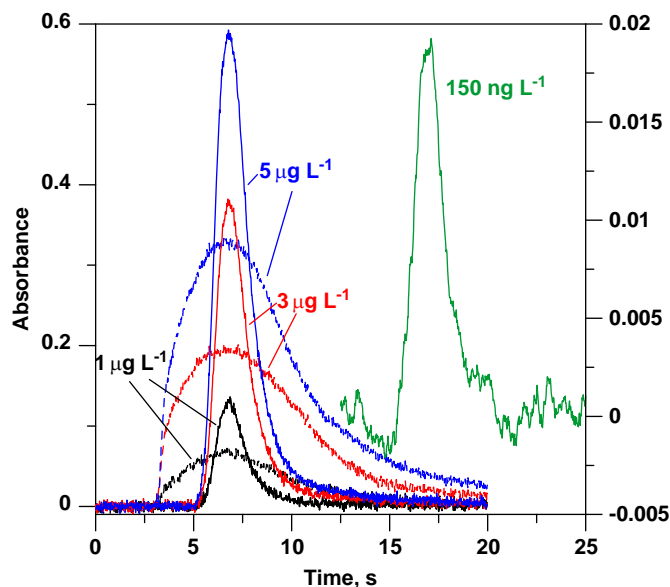


Fig. 3. Peak shape improvement using focusing by gold-plated filament (solid lines) compared to liquid phase preconcentration only (dashed lines). Right hand trace shows the signal for a  $150 \text{ ng L}^{-1}$  sample, processed with a 20-point moving average filter.

An improvement of 50-fold in detection limit was achieved. In a test of robustness, the relative standard deviation of the calibration slope was less than 4% ( $n=5$ ) over 14 days, indicating that the method is robust.

#### 3.3.5. Method validation with certified reference materials

The applicability of the present method to water samples was demonstrated by analyzing spiked samples of tap water, river water and coastal sea water. The accuracy of the method was validated with certified sub- $\mu\text{g L}^{-1}$  standard reference waters (HG95-3 and HG95-10 from Environment Canada). The data are presented in Table 2.

**Table 2**  
Determination of Hg<sup>2+</sup> in spiked samples and in certified reference materials.

Sample	Added ( $\mu\text{g L}^{-1}$ )	Found ( $\mu\text{g L}^{-1}$ ) <sup>a</sup>	Recovery (%) (% RSD)
Bangkok tap water	–	n.d.	–
	1.00	0.97 ± 0.13	97.0 (13)
	4.00	3.91 ± 0.21	97.8 (5)
River water	–	n.d.	–
	1.00	1.01 ± 0.16	97.2 (15)
	4.00	4.03 ± 0.19	99.9 (5)
Coastal sea water Chonburi	–	n.d.	–
	1.00	1.07 ± 0.22	104.3 (21)
	4.00	4.18 ± 0.16	103.7 (4)
CRM	Assigned value ( $\mu\text{g L}^{-1}$ )	Acceptable limit ( $\pm \mu\text{g L}^{-1}$ )	Found ( $\mu\text{g L}^{-1}$ ) <sup>a</sup>
HG95–3	0.157	0.0484	0.138 ± 0.028
HG95–10	0.240	0.0718	0.203 ± 0.024

n.d.: non-detectable.

<sup>a</sup> Mean ± SD ( $n=3$ ).

## Acknowledgement

This work was carried out in the Environmental Analysis Research Unit (EARU) and supported in part by Thailand Research Fund and Chulalongkorn University through the Royal Golden Jubilee Ph.D. Program (Grant PHD/37/2550), the Thailand National Research University Project of the Office of the Higher Education Commission (FW6521) and the National Research Council of Thailand (NRCT) through the High throughput screening analysis: Tool for drug discovery, disease diagnosis and health safety project. We also thank Mr. Sira Nitiyanontakit for his help with microcontroller programming.

## Appendix A. Supporting information

Supplementary data associated with this article can be found in the online version at <http://dx.doi.org/10.1016/j.talanta.2012.05.055>

## References

- [1] S. Clemens, M. Monperrus, O.F.X. Donard, D. Amouroux, T. Guerin, *Talanta* 89 (2012) 12–20.
- [2] H. Cheng, Y. Hu, *Environ. Sci. Technol.* 46 (2012) 593–605.
- [3] K. Haarstad, H.J. Bavor, T. Maehlum, *Water Sci. Technol.* 65 (2012) 76–99.
- [4] D.E.K. Dabt, D.E.J. Berger-Ritchie, G.A. McMillin, *Labmedicine* 42 (2011) 735–742.
- [5] K. Leopold, M. Foulkes, P. Worsfold, *Anal. Chim. Acta* 663 (2010) 127–138.
- [6] W. Geng, T. Nakajima, H. Takanashi, A. Ohki, *J. Hazard. Mater.* 154 (2008) 325–330.
- [7] L. Kerstin, M. Foulkes, P.J. Worsfold, *TrAC, Trends Anal. Chem.* 28 (2009) 426–435.
- [8] Y. Kalyan, S. Das, A.K. Pandey, G.R.K. Naidu, P.K. Sharma, A.V.R. Reddy, *Anal. Methods* 3 (2011) 2017–2024.
- [9] A. Moghimi, M.J. Poursharifi, *Asian J. Chem.* 23 (2011) 4117–4121.
- [10] F. Mercader-Trejo, R. Herrera-Basurto, E.R. de San, Miguel, J. de Gyves, *Int. J. Environ. Anal. Chem.* 91 (2011) 1062–1076.
- [11] Y.H. Zhai, S.E. Duan, Q. He, X.H. Yang, Q. Han, *Microchim. Acta* 169 (2010) 353–360.
- [12] K. Leopold, M. Foulkes, P.J. Worsfold, *Anal. Chem.* 81 (2009) 3421–3428.
- [13] X.-Y. Jia, D.-R. Gong, Y. Han, C. Wei, T.-C. Duan, H.-T. Chen, *Talanta* 88 (2012) 724–729.
- [14] E.M. Martinis, P. Berton, R.A. Olsina, J.C. Altamirano, R.G. Wuilloud, *J. Hazard. Mater.* 167 (2009) 475–481.
- [15] E.M. Martinis, R.G. Wuilloud, *J. Anal. At. Spectrom.* 25 (2010) 1432–1439.
- [16] S.R. Segade, J.F. Tyson, *Talanta* 71 (2007) 1696–1702.
- [17] H.-J. Zi, W.-E. Gan, S.-P. Han, X.-J. Jiang, L.-Z. Wan, *Chin. J. Anal. Chem.* 37 (2009) 1029–1032.
- [18] N.H. Khadry, A.G. Howard, *Analysis* 136 (2011) 3004–3009.
- [19] L. Zhang, X.J. Chang, Z. Hu, L.J. Zhang, J.P. Shi, R. Gao, *Microchim. Acta* 168 (2010) 79–85.
- [20] I. Lopez-Garcia, R.E. Rivas, M. Hernandez-Cordoba, *Anal. Bioanal. Chem.* 396 (2010) 3097–3102.
- [21] D.H. Anderson, J.H. Evans, J.J. Murphy, W.W. White, *Anal. Chem.* 43 (1971) 1511–1512.
- [22] J.J. McNerney, P.R. Busek, R.C. Hanson, *Science* 178 (1972) 611–612.
- [23] J.J. McNerney, *Sensors* 3 (1986) 39–41.
- [24] A. Zierhut, K. Leopold, L. Harwardt, M. Schuster, *Talanta* 81 (2010) 1529–1535.
- [25] A. Zierhut, K. Leopold, L. Harwardt, P. Worsfold, M. Schuster, *J. Anal. At. Spectrom.* 24 (2009) 767–774.
- [26] S.R. Koirtyohann, M. Khalil, *Anal. Chem.* 48 (1976) 136–139.
- [27] W.T. Corns, L. Ebdon, S.J. Hill, P.B. Stockwell, *Analyst* 117 (1992) 717–720.
- [28] M. Puanngam, S.I. Ohira, F. Unob, J.H. Wang, P.K. Dasgupta, *Talanta* 81 (2010) 1109–1115.
- [29] M. Puanngam, F. Unob, *J. Hazard. Mater.* 154 (2008) 578–587.
- [30] L. Ping, P.K. Dasgupta, *Anal. Chem.* 61 (1989) 1230–1235.
- [31] I.D. Brindle, S. Zheng, *Spectrochim. Acta B* 51 (1996) 1777–1780.
- [32] F.M. Bauzá de Mirabó, A.Ch. Thomas, E. Rubí, R. Forteza, V. Verdá, *Anal. Chim. Acta* 355 (1997) 203–210.
- [33] C. Bendicho, S. Rio-Segade, *Spectrochim. Acta B* 54 (1999) 1777–1780.
- [34] F. Ubillús, A. Alegría, R. Barberá, R. Farré, M.J. Lagarda, *Food Chem.* 71 (2000) 529–533.
- [35] J.A. Gomes Neto, L.F. Zara, J.C. Rocha, A. Santos, C.S. Dakuzaku, J.A. Nobrega, *Talanta* 51 (2000) 1129–1139.
- [36] J.F. Tyson, S. Rio Segade, *Spectrochim. Acta B* 58 (2003) 797–807.
- [37] Y. Zhang, S.B. Adeloju, *Talanta* 74 (2008) 951–957.
- [38] O. Wurl, O. Elsholz, R. Ebinghaus, *Anal. Chim. Acta* 438 (2001) 245–249.
- [39] G.P. Brandão, R.C. de Campos, A.S. Luna, *Spectrochim. Acta B* 60 (2005) 625–631.
- [40] V. Romero, I. Costas-Mora, I. Lavilla, C. Bendicho, *Spectrochim. Acta B* 66 (2011) 156–162.
- [41] M. Kan, S.N. Willie, C. Scriver, R.E. Sturgeon, *Talanta* 68 (2006) 1259–1263.
- [42] Perkin-Elmer Corp. The determination of mercury at ultratrace levels using FIMS and amalgamation technique. Technical Note, 2004. [http://www.perkinelmer.com/CMSResources/Images/44-74843TCH\\_FIMSUltraTraceMercury.pdf](http://www.perkinelmer.com/CMSResources/Images/44-74843TCH_FIMSUltraTraceMercury.pdf) Accessed May 20, 2012.
- [43] United States Environmental Protection Agency. Analytical Detection Limit Guidance. PUBL-TS-056-96, 1996. <http://dnr.wi.gov/org/es/science/lc/outreach/publications/lod%20guidance%20document.pdf>. Accessed May 20, 2012.
- [44] C.J. Patton. United States Geological Survey, Methods Development Laboratory, Denver, CO. Personal communication, May, 2012.